ZINC OXIDE NANOPARTICLES AS ADDITIVE TO ENHANCE THE SOLID-STATE EMISSION OF A HETEROLEPTIC Cu(I) COMPLEX

DANIEL NAVAS [a,*], CAMILA SANTANA [b], MIREYA SANTANDER-NELLI [c,d], LUIS SANHUEZA [e,f] ANDRÉS IBÁÑEZ [g] AND PAULINA DREYSE [h,*]

[a]Instituto de Ciencias Naturales, Facultad de Medicina Veterinaria y Agronomía, Universidad de Las Américas, Sede Providencia, Avenida Manuel Montt 948, Santiago 7500975, Chile. E-mail: daniel.navas@edu.udla.cl
[b]Departamento de Química, Universidad Técnica Federico Santa María, Av. Vicuña Mackenna 3939, San Joaquín, Chile.
[c]Advanced Integrated Technologies (AINTECH), Los Hilanderos 8521, La Reina, Santiago, Chile.
[d]Centro Integrativo de Biología y Química Aplicada (CIBQA), Universidad Bernardo O'Higgins, General Gana 1702, Santiago 8370854, Chile.
[e]Departamento de Ciencias Biológicas y Químicas, Facultad de Recursos Naturales, Universidad Católica de Temuco, Temuco, Chile.
[f]Núcleo de Investigación en Bioproductos y Materiales Avanzados (BioMA), Universidad Católica de Temuco, Av. Rudecindo Ortega 02950, Temuco, Chile.
[g]Departamento de Física, Facultad de Ciencias Físicas y Matemáticas, Universidad de Chile. Av. Beauchef 850, Santiago, Chile, Casilla 653.
[h]Departamento de Química, Facultad de Ciencia, Universidad de Chile, Las Palmeras 3425, Ñuñoa, Santiago, Chile.

ABSTRACT

The synthesis and characterization of Zinc Oxide Nanoparticles (ZnO NPs) is reported at 0°C and room temperature, with 1-octadecanol, zinc acetate and lithium hydroxide. The structural and electronic nature of the obtained ZnO NPs was confirmed by Transmission Electron Microscopy, powder X-Ray Diffraction and UV-Vis absorption. NPs exhibited diameters within 8 – 13 nm and ellipsoidal morphology.

The synergism between the ZnO NPs on the luminescent response of a Cu(I) complex in solid-state was evaluated by stacking layers on a glass substrate. Main results show that the complex increases emission response by 2.45 times compared to the absence of the ZnO NPs layer. This behaviour could be interpreted by a possible energy transfer due to the interaction between the optical band gap of ZnO NPs semiconductor with the emitting Cu(I) complex. These preliminary results suggest a close interaction between the ZnO NPs and the heteroleptic Cu(I) complex, inducing a strong emissive response on the coated glass. These results appear as outstanding to the future performance hybrid material using nanomaterials to enhance the luminescence of non-expensive metal for optical applications.

Keywords: ZnO nanoparticles, enhanced emission, heteroleptic Cu(I) complex, solid-state emission, precipitation synthesis.

1. INTRODUCTION

Among trasition metal oxide nanoparticles (NPs), ZnO NPs exhibit a wide diversity of nanostructures with highlighted optical, electrical conductor and piezoelectric properties associated with the wide energy band gap. Among the different polymorph structures of ZnO, the wurtzite structure with hexagonal unit cell, behaves as n – type semiconductor that can be classified as II – VI (12 – 16) exhibiting a superior high binding energy exciton of 60 MeV compared to other semiconductors[1,2]. Moreover, the physical properties of ZnO nanoparticles can be readily modulated through the choice of desirable synthetic methods and capping agents during their preparation[3]. In accordance with these features, ZnO NPs have been used in various technologies and industrial activities such as optoelectronics[4], piezoelectric[5], magnetic sensors[6], ceramic[7], rubber processing[8], environmental protections[9], among others.

The synthesis of ZnO NPs by chemical precipitation appears as a suitable strategy, since the obtaining of these nanoparticles can be classified as a low-energy process. Nevertheless, this strategy still requires more research to fulfill the needs for the many applications fields where they are useful. Synthetic reports include several precursors from divalent zinc salts that are usually used in ZnO NPs. Between them, zinc acetate dihydrate ($Zn(CH_3COO)_2 \bullet 2H_2O$) appears as the most used starting zinc divalent source, due to its high solubility in specific solvent mixtures, and also because this precursor is related to the corresponding outstanding performance in the morphology and size of the resulting ZnO NPs[10]. Also, this precursor reacts with different strong bases (LiOH, NaOH and KOH) producing stable ZnO NPs with wurtzite structure phase[11]. Besides, alkali hydroxides also influence the size of the ZnO NPs, promoting well-crafted nanoparticles with small size distribution and low agglomeration content[12]. For example, LiOH have been used in many ZnO NPs synthetic controllable procedures with larger surface areas[10a], obtaining spherical NPs with 10 nm average size by solvothermal treatment[13], even though it features some conglomeration[14]. By using sol – gel processes, ZnO NPs with crystalline spherical and ellipsoidal shapes have been also reported[15]. These features have inspired other synthetic procedures to generate desirable types of nanoparticles, for example, including solvothermal treatments at different temperatures[16].

On the other hand, it is well-known that coordination compounds with metals from the second and third transition series, have excellent luminescent properties, which have been used in lighting technologies[17], sensing[18], as potential drugs for anticancer therapy[19], among others. Although the luminescence of these types of complexes offers great benefits, there are some drawbacks regarding the highly synthetic costs since expensive and scarce metals are usually involved, namely: Pt, Ru, Ir, Re, Os, and others. In this context, despite the lower emissive performance, coordination complexes involving more abundant transition metals from the first row appears attractive. Of these, copper appears as a desired metal since in the 1+ oxidation state affords tetrahedral complexes with intriguing luminescent properties that could be used to replace the complexes including metals of the second and third series[20]. However, the relative lower luminescent performance of Cu(I) complexes compared, for instance, to the outstanding emission of Ru or Ir complexes limit the use of Cu complexes for desirable applications. In this sense, considering the electronic and structural properties of ZnO NPs interaction between a poorly luminescent coordination complex, for instance, in Cu(I) complexes and ZnO nanoparticles appears attractive to induce a synergism on the emission properties. Despite these studies are scarce in the literature, there are some antecedents of increased electroluminescence of Ir(III) complexes by the effect of bulk ZnO and ZnO nanoparticles[21]. Besides, some studies of porphyrin−ZnO NPs assemblies explain this effect by an energy transfer[22] or by the hindrance of the rotational relaxation of porphyrin producing by the ZnO NPs to generate fluorescence increment[23]. Another approach has been the role of ZnO as an emission enhancer in Mn^{2+}-doped ZnS/ZnO composite phosphors, where ZnO functions as a wide-bandgap host with strong UV absorption, promoting efficient exciton generation, and defect-assisted luminescence pathways that facilitate energy transfer to Mn^{2+} centers, producing broad and intense visible emission[24]. Nevertheless, studies of increased luminescence in solution or solid state have not been detailed studied for ZnO NPs / Cu(I) complexes.

This work shows the synthesis of ZnO NPs under mild chemical conditions (performed at 0°C and room temperature), using $Zn(CH_3COO)_2 \bullet 2H_2O$, LiOH, and 1-octadecanol as a low-cost long hydrocarbon chain neutral surfactant. The obtained ZnO NPs were structurally characterized through X-Ray Diffraction (XRD), Transmission Electron Microscopy (TEM) and Infrared spectroscopy

*Corresponding author email: paulinadreyse@uchile.cl

(FT – IR). In addition, UV–Vis absorption spectroscopy and diffuse reflectance spectroscopy (DRS) were used to evaluate the optical electronic characterization. To study the effect of the ZnO NPs on the enhanced emission of a Cu-based emitter, a heteroleptic Cu(I) complex of the type [Cu(BCP)(POP)](PF_6), where BCP = bathocuproine or 2,9-dimethyl-4,7-diphenyl-1,10-phenanthroline and POP = bis-[2-(diphenylphosphino)-phenyl]ether, was considered. The interaction was achieved by spin coating technique on a Corning® glass surface was modified with a ZnO NPs layer from 1–hexanol suspension and then covered with the Cu(I) complex layer in acetonitrile solution. Enhanced emissions were evidenced in all measurements carried out, showing in the best case an increase up to 145%.

2. EXPERIMENTAL

2.1. Materials and Reagents

All reagents and solvents used in this work, including zinc acetate dihydrate ($Zn(CH_3COO)_2•2H_2O$), 1-octadecanol 95%, ethanol, methanol, lithium hydroxide (LiOH), 1–hexanol, acetonitrile and double deionized water were used were of analytic grade from Merck. The heteroleptic Cu(I) complex was prepared according to previous reported methods where characterization was in complete agreement with reference data[25].

The ZnO nanoparticles were synthesized following previous reported methods,[10a, 26] to obtain desirable NPs with spherical morphology and dimensions less than 10 nm, conducted by 1-octadecanol. This strategy followed a similar precipitation route, using two different temperatures at 0°C (using an ice bath) or 25°C (room temperature) and several washing steps. Indistinctly, 25 mL of an ethanolic solution 0.050 M $Zn(CH_3COO)_2•2H_2O$ was added in a 100 mL round bottom flask. Then, 1.13 mmol of 1-octadecanol dissolved in 25 mL of methanol was slowly added under continuous stirring and the resulting mixture stirred vigorously for 1 hour. After this time, the precipitation process was performed by dropping 25 mL of 0.1 M ethanolic solution of LiOH, and the resulting mixture was vigorously stirred for 4 hours. The resulting ZnO NPs crude mixture was treated for this process: the ethanol / methanol mixture was evaporated first, then the solid was washed several times with acetone under constant agitation, and finally the precipitated ZnO NPs were separated from the acetone / 1-octadecanol mixture by decantation. The ZnO NPs were dried at 80°C and stored in dry conditions.

2.2. Characterization of ZnO NPs

The structural characterization of the powders ZnO NPs was made with XRD technique using a SIEMENS D 5000 diffractometer (Cu Kα, λ = 1.54 Å, operation voltage 40 kV, current 30 mA). Besides, the ZnO NPs morphology was characterized using Transmission Electron Microscopy (TEM), model Hitachi HT7700 High-resolution. Here, the ZnO NPs samples were previously suspended in absolute ethanol and dropped on a TEM grid and left to dry at room temperature. Zn – O bonds were characterized using FT-IR spectroscopy in a Jasco FT/IR – 4600 equipment in KBr pellets in the region 4000 – 240 cm^{-1}. The electronic characterization was carried out by UV-Vis absorption spectroscopy, in a Thermo Scientific model evolution 220 spectrophotometer; the samples were measured using ethanol nanoparticles suspensions in a range from 200–750 nm. The optical band gaps for each ZnO powders were determined in a Jasco V-750 spectrophotometer with an integrating sphere (Spectralon reference tile cap). Experiments were recorded between 200-800 nm, at 200 nm/min scan rate using Reflectance measurements were transformed to absorption spectra using the Kubelka-Munk function[27].

2.3. ZnO NPs – Cu(I) complex interactions and luminescent characterization

A Corning® glass surface of 0.80 (length) and 4.5 (width) cm dimensions was used as the substrate for modifications, where layers composed by ZnO NPs and Cu(I) complex were spin coated on the substrate according to the following procedure: first: The colorless thin ZnO layer was prepared using 5.0 mg/mL of ZnO NPs (synthesis performed at 0°C) suspended in 1–hexanol; the suspension was previously stirred by ultrasound bath for 1.5 h, and 20 µL aliquot was added on the Corning® glass by spin coating using the following protocol: i) 500 rpm for 30 s to add the aliquot; ii) 1000 rpm for 30 s to spread the aliquot; and iii) finally 60 s at 2500 rpm to volatilize the solvent. After coating the ZnO NPs layer, 20 µL of a 5.0 mg/mL Cu(I) complex in acetonitrile solution was deposited over the ZnO layer obtaining a yellow-colored layer of the Cu(I) complex, by using the same procedure explained for ZnO NPs. Once the modification was performed, the emission spectra was measured immediately. To compare the results, two Corning® blanks were prepared and measured; one blank glass exclusively with ZnO NPs using spin coating technique, and the other blank glass solely with the Cu(I) complex, using the same parameters previously mentioned.

3. RESULTS AND DISCUSSION

3.1. Synthesis and characterization of the ZnO NPs

The whole synthetic procedure was designed to obtain ZnO NPs under mild chemical conditions. Considering both temperatures used in the synthesis (i.e. 0°C and room temperature), the obtained ZnO NPs did not promote noticeably differences in the obtained NPs, nor the observed polydispersity. The only detectable effect was a slower precipitation reaction at 0°C. Here, the ZnO were obtained under an ethanol/methanol mixture to allow easy solubilization of 1-octadecanol, therefore, the precipitation took place between the surfactant arrangement in which the nucleation process was quickly stabilized by the surfactant, as a key effect on the nanoparticle formation. Besides, as previously reported, the LiOH has been used generally to originate small ZnO NPs with high crystallinity[28]. Regarding the metallic precursor, $Zn(CH_3COO)_2•2\,H_2O$ has been used in a wide range of ZnO NPs syntheses because it generates ZnO in multiple steps mechanism, where ZnO is not formed abruptly due to the participating effect of the acetate counterion; i.e., when pH is being increased by adding the base, therefore, the growth of the NPs can be controlled[29].

Considering the synthetic conditions, the whole process of nanoparticle formation can be described as follows:

$$Zn(CH_3COO)_2 \bullet 2H_2O + 2\,LiOH \xrightarrow{1-octadecanol} ZnO + 2\,CH_3COOLi + 3\,H_2O$$

According to the literature[30], the ZnO NPs formation could be related to a three step stages: i) The first stage corresponds to the precipitation of $Zn(OH)_2$ once the pH slowly increases, this should be happening under strong agitation in presence of 1-octadecanol, which might be participating in the control of the precipitation rate adopting a certain geometric configuration in between the polar solvents (ethanol and water from the hydrated salt) and the ionic precursor (Zn^{2+} and CH_3COO^-). This stage concludes after adding LiOH and a white precipitate appears. ii) The second stage involves the ZnO formation, in a basic and stabilized pH, where zinc hydroxides yields ZnO NPs likely in multiple mechanisms, as previously reported in sol – gel processes reported by Meulenkamp[31]. iii) The final stage could be taking place in synchronicity with the previous stage[32], concealed by reactions between zinc hydroxide with the $Zn(CH_3COO)_2•2\,H_2O$ precursor to produce ZnO NPs.

To gain insights into the structural characterization of the obtained ZnO-NPs, powder XRD analysis was performed to observe the effect of the different temperatures on the nanoparticle morphology. As shown in Figure 1, all XRD patterns have the same diffraction peaks (independent of the temperature used in the synthesis), attributed to Zincite (ZnO, JCPDS card 36 – 1451) with hexagonal phase lattice unit cell associated to wurtzite structure, with red parameters a = 0.3249 nm and c = 0.5206 nm, and a $p6_{3mc}$ space group. Comparison with the pattern confirms that there are no other crystalline reflection peaks, exhibiting a solely ZnO phase.

As observed in Figure 1, the peak intensities obtained at room temperature are higher than those of the samples obtained at 0°C. This behavior can be attributed to the sample crystallinity that might have decreased at low temperature probably because 1-octadecanol was restricted to interact freely with other species by generating or adopting a self-organized disposition, at the same time at room temperature the surfactant could have adopted some degree of self-assembly which induced an increase in the crystallinity of the synthesized nanoparticles[33]. Another distinctive feature is the 101 peak intensity, which is usually reported in the literature[34] as the preferential growing direction plane during the ZnO NPs formation, being this peak observed with a high intensity in all XRD characterizations of the ZnO NPs synthesized.

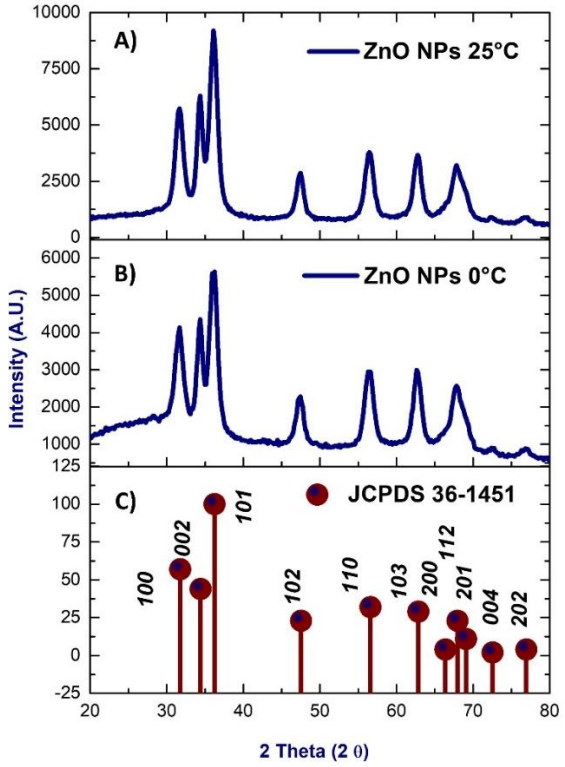

Fig. 1. ZnO NPs structural characterizations by XRD technique. A) ZnO NPs at 25°C, B) ZnO NPs at 0°C, and C) JCPDS 36-1451 pattern.

To characterize the morphology and size of the synthesized ZnO NPs, transmission electron microscopy (TEM) was also considered. As shown in Figure 2, the micrograph displays small ZnO NPs with similar morphology; ellipsoidal and spherical shapes are observed, with diameters ranging in between 6 to 14 nm, respectively. This result also shows that the temperature used for both syntheses might not be a critical parameter in terms of size and morphology. For instance, the histogram of ZnO NPs obtained from the TEM image of the synthesis at 0°C shows a size distribution with diameters ranging from 8 to 11 nm; the most significant frequency in terms of diameter sizes is 19% approximately, with diameters ranging between 9 and 10 nm, although diameters from 8 to 9 and 10 to 11 nm are also relevant displaying a 16% frequency, showing a similar tendency at 25°C.

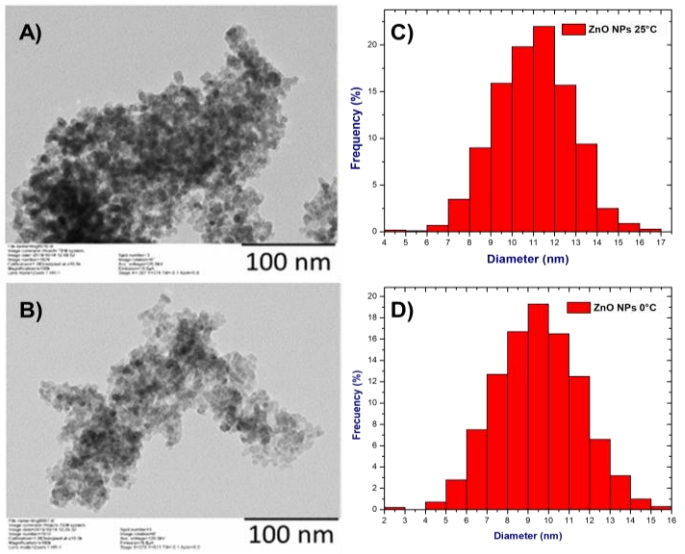

Fig. 2. TEM images of: A) ZnO NPs synthetized at 25°C and B) synthetized at 0°C. The corresponding histogram of: C) ZnO NPs synthetized at 25°C and D.) at 0°C.

Besides, FT – IR spectroscopy was used to identify the presence of Zn–O vibrational modes and vibrations from 1-octadecanol and acetate ion residuals. Figure 3 exhibits the infrared spectrum of ZnO NPs obtained at 25°C (spectrum at 0°C does not show substantial differences; the comparative spectra can be observed in the Figure S.1 and table S.1 of the Supporting Information).

As well as in the XRD analysis, all infrared spectra for the obtained ZnO NPs exhibit the same pattern, namely, there are bands associated to the presence of 1-octadecanol according to the presence of vibrational mode at 3500 cm^{-1} of the O–H bond, residual CH_3COO^- stretching modes are also detectable at 1563, 1430 cm^{-1} and 845 cm^{-1}, besides the stretching and bending vibrational modes of C–H bonds are displayed at high and medium wavenumbers of the spectra. The Zn–O vibrational modes are registered in the 450 to 550 cm^{-1} range. In this case, several vibrational bands appear, associated to nanometric ZnO with different Zn–O bonds strengths. This effect results in a wide sharp peak instead as an average of all these stretching Zn–O vibrations[33, 35].

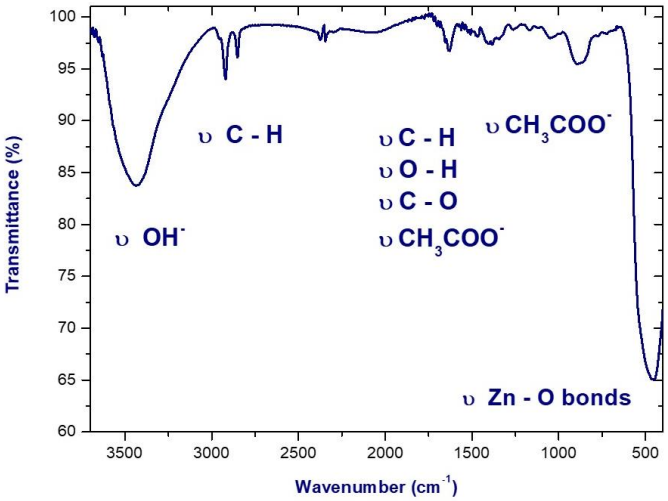

Fig. 3. FT-IR spectrum of ZnO NPs at 25°C in KBr pellet.

The normalized UV-Vis spectra of the ZnO NPs obtained are shown in Figure 4. Here, at both temperature, a maximum absorption appearing at 353 nm; blue shifted in comparison with other reported ZnO NPs (λ = 365 nm)[36].

The diffuse reflectance analysis of ZnO NPs was also determined, showing a slight energy difference between the 3.25 eV optical band gap value with the synthesis performed at 0°C and 3.31 eV band gap value for the synthesis at 25°C (See supporting information, Figure S.3.). These values agree with previously reported values in the range of 3.30 to 3.27 eV for similar nanostructures, obtained by increasing temperature treatment from 300 to 700°C, respectively[37]. Noticeably, in our case, the decreased optical band gap values afford in terms of decreasing the temperature conditions. These observations could be related to the specific synthetic protocol, as well as the kinetic control during the nanoparticle formation due to oxygen vacancies lattice defects that diminish the band gap and are raised as consequences from the precipitation processes[38].

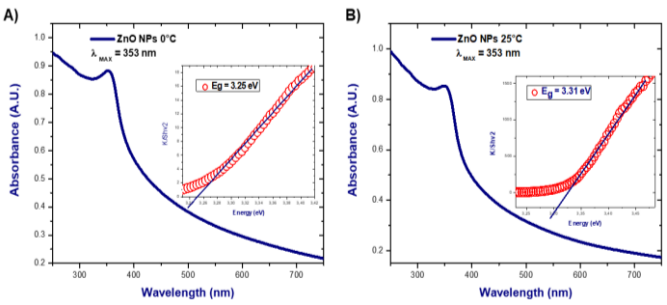

Fig. 4. Normalized absorption spectrum and diffuse reflectance band gap calculation with Kubelka-Munk function for the obtained ZnO NPs at A) 0°C and B) 25°C, all measured in ethanolic suspension.

3.2. Enhanced emission of Cu(I) complex by ZnO NPs

To study the effect of the obtained ZnO NPs onto the luminescent properties of Cu(I) complexes, a series of experiments were performed to achieve the modulation of the emission response of the [Cu(BCP)(POP)](PF_6) complex. This complex was considered as object of study since low-cost and abundant raw-materials, including metals from the first-row transition series have been highly demanding to replace the more scarce and expensive luminescent materials, such as Iridium, Osmium, between others.[39] The Cu(I) complex was successfully prepared by conventional synthetic methods and the characterization was in complete agreement with previous reported data[25, 40]. Also, considering the potential use of Cu(I) complexes as luminescent materials in lighting devices, the electronic deactivation response was studied in solid state, by spin-coating technique on a Corning® glass surface at room temperature.

The emission spectrum of the Cu(I) complex deposited onto glass surface is depicted in Figure 5 (red line). This spectrum was obtained under excitation at 360 nm which correspond to the wavelength associate with the metal to ligand charge transfer process, showing an emission maximum at 559 nm, consistent with the emission report for this complex in solution and in the solid-state[25, 40]. The emission of the Cu(I) complex was performed in multiple tests and did not show any change as an indicative of the stable behavior of the complex in solid-state. Comparing the emissive behavior of the isolated compounds, the solid-state emission spectrum of isolated ZnO NPs was performed by spin-coating a layer of ZnO NPs prepared at 0°C in different surfaces. After exciting at the same wavelength (λ_{ex} = 360 nm) the ZnO NPs do not showed any emission response at the excitation wavelength used (see Supporting Information Figure S.2.) in complete agreement with literature data since this type of NPs show an emissive behavior in the blue and green region between 415 - 488 nm[41].

The solid-state emission corresponding to the interaction of the bilayer composed by the heteroleptic Cu(I) complex film onto the ZnO NPs layer was obtained under excitation at 360 nm and appears in Figure 5 in the blue line. By comparing both spectra, clearly the emission of the Cu(I) is significatively increased, in this case by a factor of 2.45 with respect to the emission of the Cu(I) complex without NPs. These observed emissive modulation could be related to some possible energy transfer from ZnO NPs to luminescent Cu(I) compound, due to the high band gap of the ZnO NPs of small size, as previously reported in literature for similar experiments[22]. Recent studies on ZnO–carbon hybrid nanomaterials made by Sreenan *et al* demonstrate that embedding ultrasmall ZnO nanoparticles (2–5 nm) within a carbon matrix creates unique luminescence behavior due to strong interfacial interactions between ZnO defect states and carbon-based localized electronic states. This coupling produces dual emission pathways, significantly enhancing photoluminescence quantum yield and stability. Analogously, when ZnO is applied as an additive in Cu(I) complexes, its excitonic states and surface defect levels can couple with the metal-to-ligand charge transfer (MLCT) states of Cu(I), enabling new energy transfer routes and suppressing non-radiative deactivation. Moreover, the stabilizing effect of ZnO may mitigate the intrinsic instability of Cu(I) complexes, thereby amplify their emission[42]. In addition, the emission-enhancing role of ZnO has been extensively demonstrated and reviewed by Sood *et al* in rare-earth–doped systems, where the incorporation of ions such as Eu^{3+}, Tb^{3+}, or Dy^{3+} introduces intermediate states within the ZnO bandgap that couple effectively with host excitons and defect levels, resulting in bright, tuneable, and long-lived luminescence.

To obtain additional insights about the observed results, the reproducibility of the increased emission for the prepared Cu/ZnO NPs solid luminescent layer was tested. Here, a series of different surfaces were obtained and measured in the same conditions. In all cases, the sample with ZnO NPs/Cu(I) complex showed an increased emission compared to the layer with only Cu(I) complex (see Supporting Information; Figure S.3.). Although the reproducibility of the emission intensity is still under study, the increased emission reached values between 1.79 to 2.45 times compared to the isolated Cu(I) layer. There is well known that, in general terms, the different layer deposition must be carefully controlled in order to obtain good reproducibility in the corresponding properties, since there are several parameters to control the non-covalent interactions that can occur during the layer arrangements.[44] In our case, believe that the observed reproducibility could be improved by a more thorough study of the experimental conditions used in spin coating, or by changing the coating technique for depositing the NPs layer, since in many cases holes and/or agglomerations hinder the formation of homogeneous coated surfaces, which may limit increased emissions. Despite this reproducibility issue, the results presented in this study constitute an outstanding precedent, showing the advantage of the synthesized NPs in enhancing the emission of a Cu(I) complex.

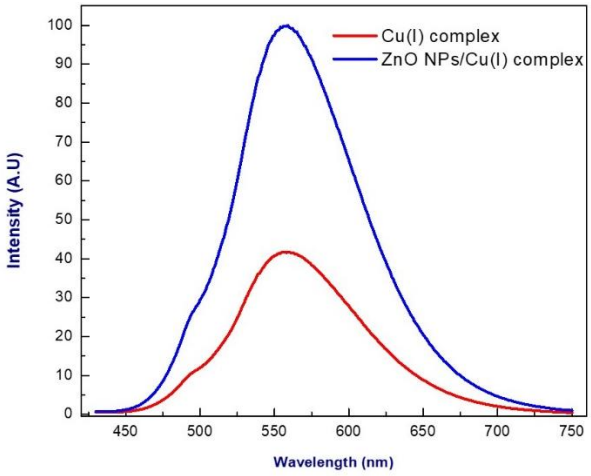

Fig. 5. Emission spectra in solid-state (glass surface) of Cu(I) complex layer and ZnO NPs / Cu(I) complex layer.

CONCLUSION

ZnO NPs were successfully synthesized in simple way, avoiding hard experimental conditions, using with 1-octadecanol as surfactant, obtaining desired nanoparticles display an ellipsoidal morphology and a good size distribution. These NPs were used to modify a glass surface and to generate a bilayer obtaining an interaction of ZnO NPs layer / Cu(I) complex, which presented increased emission compared to the glass covered only with Cu(I) complex in the same experimental conditions. The enhanced emission reached up to 2.45 times the emissive response of the isolated Cu(I) layer, attributable by energy transfer process due to the interaction between the wide band gap of ZnO NPs semiconductor with the emitting Cu(I) complex.

Despite the homogeneity improvement of the NPs layer for a reproducible response was not deeply studied in this work, these results appear as a valuable precedent to maximize the emissive response of a poorly luminescent surface towards its implementation on electronic and optoelectronic. Although the emission in Cu(I) complexes is usually characterized by low quantum yield, the intriguing electronic structure of this type of molecules places these systems as strategic in optoelectronic applications, such as lighting devices and sensors. Therefore, the assembly of ZnO NPs / Cu(I) complex would allow to be a powerful alternative to the expensive second and third row metallic coordination compounds currently leader in the luminescent properties.

ACKNOWLEDGMENTS

M. S-N. acknowledges to FONDECYT project N°3170663, P. D. acknowledges to FONDECYT project N°1201173 and PI_M_2020_31 USM project, L. S. acknowledges to FONDECYT project Nº 11181187.

REFERENCES

[1] a) K. Davis, R. Yarbrough, M. Froeschle, J. White and H. Rathnayake, *RSC Advances* **2019**, *9*, 14638-14648; b) M. Carofiglio, S. Barui, V. Cauda and M. Laurenti, *Applied Sciences* **2020**, *10*, 5194.

[2] a) Y. F. Zhu and W. Z. Shen, *Applied Surface Science* **2010**, *256*, 7472-7477; b) A. Moballegh, H. R. Shahverdi, R. Aghababazadeh and A. R. Mirhabibi, *Surface Science* **2007**, *601*, 2850-2854.

[3] T. Vu Anh, T. A. T. Pham, V. H. Mac and T. H. Nguyen, *Journal of Analytical Methods in Chemistry* **2021**, *2021*, 5533734.

[4] N. Bano, I. Hussain, S. Aodah and M. S. AlSalhi, *Materials Research Express* **2019**, *6*, 115629.

[5] M. Manikandan, P. Rajagopalan, N. Patra, S. Jayachandran, M. Muralidharan, S. S. Mani Prabu, I. A. Palani and V. Singh, *Nanotechnology* **2020**, *31*, 185401.

[6] M. A. Subhan, P. C. Saha, M. M. Alam, A. M. Asiri, M. Al-Mamun and M. M. Rahman, *Journal of Environmental Chemical Engineering* **2018**, *6*, 1396-1403.
[7] M. Sheikh, M. Pazirofteh, M. Dehghani, M. Asghari, M. Rezakazemi, C. Valderrama and J.-L. Cortina, *Chemical Engineering Journal* **2020**, *391*, 123475.
[8] Z. Xu, L. Zheng, S. Wen and L. Liu, *Composites Part A: Applied Science and Manufacturing* **2019**, *124*, 105492.
[9] E. A. S. Dimapilis, C.-S. Hsu, R. M. O. Mendoza and M.-C. Lu, *Sustainable Environment Research* **2018**, *28*, 47-56.
[10] a) Y. Lv, W. Xiao, W. Li, J. Xue and J. Ding, *Nanotechnology* **2013**, *24*, 175702; b) A. Moezzi, A. McDonagh, A. Dowd and M. Cortie, *Inorganic Chemistry* **2013**, *52*, 95-102; c) M. N. Shamhari, S. B. Wee, F. S. Chin and Y. K. Kok, *Acta chimica Slovenica* **2018**, *65 3*, 578-585; d) R. K. Sharma and R. Ghose, *Ceramics International* **2015**, *41*, 967-975.
[11] a) V. Koutu, L. Shastri and M. M. Malik, *Materials Science-Poland* **2016**, *34*, 819-827; b) K.-K. Liu, C.-X. Shan, R. Zhou, Q. Zhao and D.-Z. Shen, *Optical Materials Express* **2017**, *7*, 2682-2690.
[12] S. Gyawali, L. K. M. O. Goni, M. S. Chowdhury, A. Laref, S. Bajgai, S. Chantrapromma and K. Techato, *Materials Research Express* **2022**, *9*, 055004.
[13] Q. R. Hu, S. L. Wang and W. H. Tang, *Materials Letters* **2010**, *64*, 1822-1824.
[14] M. Makkar and H. S. Bhatti, *Chemical Physics Letters* **2011**, *507*, 122-127.
[15] A. Sharma, B. P. Singh, S. Dhar, A. Gondorf and M. Spasova, *Surface Science* **2012**, *606*, L13-L17.
[16] a) Y. Im, S. Kang, B. S. Kwak, K. S. Park, T. W. Cho, J.-S. Lee and M. Kang, *Korean Journal of Chemical Engineering* **2016**, *33*, 1447-1455; b) W. Widiyastuti, S. Machmudah, T. Nurtono, S. Winardi, R. Balgis, T. Ogi and K. Okuyama, *Chemical Engineering Transactions* **2017**, *56*, 955-960.
[17] a) F. Brunner, L. Martínez-Sarti, S. Keller, A. Pertegás, A. Prescimone, E. C. Constable, H. J. Bolink and C. E. Housecroft, *Dalton Transactions* **2016**, *45*, 15180-15192; b) M. J. Leitl, V. A. Krylova, P. I. Djurovich, M. E. Thompson and H. Yersin, *Journal of the American Chemical Society* **2014**, *136*, 16032-16038; c) S. Keller, F. Brunner, J. M. Junquera-Hernández, A. Pertegás, M.-G. La-Placa, A. Prescimone, E. C. Constable, H. J. Bolink, E. Ortí and C. E. Housecroft, *ChemPlusChem* **2018**, *83*, 217-229.
[18] a) A. O. Razgoniaev, C. E. McCusker, F. N. Castellano and A. D. Ostrowski, *ACS Macro Letters* **2017**, *6*, 920-924; b) A. Singh, A. Singh, N. Singh and D. O. Jang, *Sensors and Actuators B: Chemical* **2017**, *243*, 372-379.
[19] V. Gandin, C. Ceresa, G. Esposito, S. Indraccolo, M. Porchia, F. Tisato, C. Santini, M. Pellei and C. Marzano, *Scientific Reports* **2017**, *7*, 13936.
[20] a) M. W. Mara, K. A. Fransted and L. X. Chen, *Coordination Chemistry Reviews* **2015**, *282-283*, 2-18; b) Y. Zhang, M. Schulz, M. Wächtler, M. Karnahl and B. Dietzek, *Coordination Chemistry Reviews* **2018**, *356*, 127-146; c) C. Minozzi, A. Caron, J.-C. Grenier-Petel, J. Santandrea and S. K. Collins, *Angewandte Chemie International Edition* **2018**, *57*, 5477-5481; d) J. Kim, D. R. Whang and S. Y. Park, *ChemSusChem* **2017**, *10*, 1883-1886.
[21] M. D. Marcantonio, S. Gellner, J. E. Namanga, J. Frohleiks, N. Gerlitzki, F. Vollkommer, G. Bacher and E. Nannen, *Advanced Materials Technologies* **2017**, *2*, 1600215.
[22] a) I. Hiromitsu, T. Ikeue, K. Karino, T. Ohno, S. Tanaka, H. Shiratori, S. Morito, Y. Fujita and M. Handa, *Chemical Physics Letters* **2009**, *474*, 315-319; b) I. Hiromitsu, A. Kawami, S. Tanaka, S. Morito, R. Sasai, T. Ikeue, Y. Fujita and M. Handa, *Chemical Physics Letters* **2011**, *501*, 385-389.
[23] S. M. B. Aly, M. Eita, J. I. Khan, E. Alarousu and O. F. Mohammed, *The Journal of Physical Chemistry C* **2014**, *118*, 12154-12161.
[24] H. G. Chuc, P. M. Tri, M. T. Tran, D. Q. Trung, N. Tu, N. Van Du, N. M. Hieu, N. D. T. Kien, T. N. Bach, L. T. Ha, N. D. Hung, D. X. Viet, N. N. Ha, P. T. Huy, *RSC Adv.*, **2025**,*15*, 26027-26038.
[25] N. Armaroli, G. Accorsi, M. Holler, O. Moudam, J.-F. Nierengarten, Z. Zhou, R. T. Wegh and R. Welter, *Advanced Materials* **2006**, *18*, 1313-1316.
[26] a) S. Daumann, D. Andrzejewski, M. Di Marcantonio, U. Hagemann, S. Wepfer, F. Vollkommer, G. Bacher, M. Epple and E. Nannen, *Journal of Materials Chemistry C* **2017**, *5*, 2344-2351; b) D. P. Singh, *Science of Advanced Materials* **2010**, *2*, 245-272.
[27] D. Kumar and S. Pal, *AIP Conference Proceedings* **2019**, *2142*.
[28] H.-M. Xiong, R.-Z. Ma, S.-F. Wang and Y.-Y. Xia, *Journal of Materials Chemistry* **2011**, *21*, 3178-3182.
[29] G. Rajendran, S. P. Datta, R. D. Singh, S. C. Datta and M. Vakada, *Inorganic and Nano-Metal Chemistry* **2022**, *52*, 185-194.
[30] X-F. Huang, F-F. Ju, M-Z. Wang, X-W. Ge, *Chinese Journal of Chemical Physics* **2012**, *25*, 719.
[31] E. A. Meulenkamp, *The Journal of Physical Chemistry B* **1998**, *102*, 5566-5572.
[32] S. Mustapha, M. M. Ndamitso, A. S. Abdulkareem, J. O. Tijani, D. T. Shuaib, A. K. Mohammed and A. Sumaila, *Advances in Natural Sciences: Nanoscience and Nanotechnology* **2019**, *10*, 045013.
[33] H. Heinz, C. Pramanik, O. Heinz, Y. Ding, R. K. Mishra, D. Marchon, R. J. Flatt, I. Estrela-Lopis, J. Llop, S. Moya and R. F. Ziolo, *Surface Science Reports* **2017**, *72*, 1-58.
[34] M. Saleem, A. Manzoor, M. Zaffar, S. Z. Hussain and M. S. Anwar, *Applied Physics A* **2016**, *122*, 589.
[35] O. Bundit and K. Wongsaprom, *Journal of Physics: Conference Series* **2018**, *1144*, 012044.
[36] P. A. Rodnyi and I. V. Khodyuk, *Optics and Spectroscopy* **2011**, *111*, 776-785.
[37] S. S. Kumar, P. Venkateswarlu, V. R. Rao and G. N. Rao, *International Nano Letters* **2013**, *3*, 30.
[38] L.-l. Chen, B.-g. Zhai and Y. M. Huang, *Catalysts* **2020**, *10*, 1163.
[39] Y. Liu, S.-C. Yiu, C.-L. Ho and W.-Y. Wong, *Coordination Chemistry Reviews* **2018**, *375*, 514-557.
[40] M. Santander-Nelli, L. Sanhueza, D. Navas, E. Rossin, M. Natali and P. Dreyse, *New Journal of Chemistry* **2022**, *46*, 1693-1703.
[41] H. Zeng, G. Duan, Y. Li, S. Yang, X. Xu and W. Cai, *Advanced Functional Materials* **2010**, *20*, 561-572.
[42] B. Sreenan, V. Kafil, T. Hunt, S. H. Ra Shin, A. A. Brennan, P. K. Thallapally, Y. Tal-Gan, X. Zhu, *ACS Appl. Opt. Mater.* **2025**, *3*, 3, 698–711.
[43] S. Sood, P. Kumar, I. Raina, M. Misra, S. Kaushal, J. Gaur, S. Kumar, G. Singh, *Photonics* **2025**, *12*, 454.
[44] a) S.-Y. Pung, K.-L. Choy, X. Hou and C. Shan, *Nanotechnology* **2008**, *19*, 435609; b) V. Myndrul, L. Vysloužilová, A. Klápšťová, E. Coy, M. Jancelewicz and I. Iatsunskyi, *Coatings* **2020**, *10*, 1199; c) P. Boryło, K. Matus, K. Lukaszkowicz, J. Kubacki, K. Balin, M. Basiaga, M. Szindler and J. Mikuła, *Applied Surface Science* **2019**, *474*, 177-186; d) R. Kumar, G. Kumar, O. Al-Dossary and A. Umar, *Materials Express* **2015**, *5*, 3-23.